Optimization of Temperature Sensitivity Using the Optically Detected Magnetic-Resonance Spectrum of a Nitrogen-Vacancy Center Ensemble

Kan Hayashi,[1,2,3,*] Yuichiro Matsuzaki,[3] Takashi Taniguchi,[4] Takaaki Shimo-Oka,[1] Ippei Nakamura,[2,†] Shinobu Onoda,[5] Takeshi Ohshima,[5] Hiroki Morishita,[1] Masanori Fujiwara,[1] Shiro Saito,[3] and Norikazu Mizuochi[1]

[1]*Institute for Chemical Research, Kyoto University, Uji, Kyoto 611-0011, Japan*
[2]*Graduate School of Engineering Science, Osaka University, Toyonaka, Osaka 560-8531, Japan*
[3]*NTT Basic Research Laboratories, NTT Corporation, Atsugi, Kanagawa 243-0198, Japan*
[4]*National Institute for Materials Science, Tsukuba, Ibaraki 305-0044, Japan*
[5]*National Institutes for Quantum and Radiological Science and Technology, Takasaki, Gunma 370-1292, Japan*

(Received 20 February 2018; revised manuscript received 24 May 2018; published 6 September 2018)

Temperature sensing with nitrogen-vacancy (NV) centers using quantum techniques is very promising, and further development is expected. Recently, the optically detected magnetic-resonance (ODMR) spectrum of a high-density ensemble of NV centers was reproduced with noise parameters [inhomogeneous magnetic field, inhomogeneous strain (electric field) distribution, and homogeneous broadening] of the NV center ensemble. In this study, we use ODMR to estimate the noise parameters of the NV centers in several diamonds. These parameters strongly depend on the spin concentration. This knowledge is then applied to theoretically predict the temperature sensitivity. Using the diffraction-limited volume of 0.1 μm^3, which is the typical limit in confocal microscopy, we estimate the optimal sensitivity to be around 0.76 mK/$\sqrt{\text{Hz}}$ with an NV center concentration of 5.0×10^{17}/cm^3. This sensitivity is much higher than previously reported sensitivities, demonstrating the excellent potential of temperature sensing with NV centers.

DOI: 10.1103/PhysRevApplied.10.034009

I. INTRODUCTION

A negatively charged nitrogen-vacancy (NV) center in diamond [1,2] is a promising system to realize practical quantum devices [3–23]. The spin state of a NV center can be initialized, manipulated, and read out at room temperature [3,4]. Because of the excellent controllability and long coherence time [19–21], entanglement generation between NV centers has already been demonstrated [3–11]. These techniques have been applied to NV centers for quantum-information processing [3–6], quantum hybrid devices [22–24], and quantum sensing [7–18]. In particular, single NV centers have been used to detect magnetic fields [7–11], temperature [11–14], pressure [15], and electric fields [16–18] on the nanometer scale. Not only a single NV center but also a high-density ensemble of NV centers have been studied for quantum-sensing applications. Because the sensitivity increases by $\sqrt{N}$ as the number of NV centers contributing to measurements (N) increases, an ensemble of NV centers is expected to be a suitable high-sensitivity sensor with a spatial resolution on the submicron to millimeter scale. Because of various potential applications, the basic properties of a NV center ensemble have been intensively studied [7,24–28].

A NV center constitutes a spin-1 system in the ground-state manifold. Figure 1 shows its energy diagram. The $|m_s = 0\rangle$ and $|m_s = \pm 1\rangle$ levels are split by axial zero-field splitting, $D_g \approx 2.87$ GHz. Without an applied magnetic field, the energy eigenstates are described as $|B\rangle = (1/\sqrt{2})(|1\rangle + |-1\rangle)$ and $|D\rangle = (1/\sqrt{2})(|1\rangle - |-1\rangle)$, where these two states are energetically split by the strain (electric) fields. On the other hand, on application of an external magnetic field B larger than the strain (electric) field, the energy eigenstates are $|m_s = \pm 1\rangle$, and these states are separated by the Zeeman energy of $2g_e\mu_B B$, where $g_e = 2.003$ is the NV center g factor and μ_B is the Bohr magneton. The NV center spin state can be optically initialized as $|m_s = 0\rangle$, and measurement of the spin-dependent fluorescence can give the spin states. Hence, the magnetic resonance between the energy eigenstates in the ground-state manifold can be detected optically. From the resonant frequencies of the optically detected magnetic resonance (ODMR), the temperature, magnetic fields, and electric fields can be estimated.

*hayashi@dia.kuicr.kyoto-u.ac.jp
†Present address: RIKEN Center for Emergent Matter Science (CEMS), Wako, Saitama, 351-0198, Japan

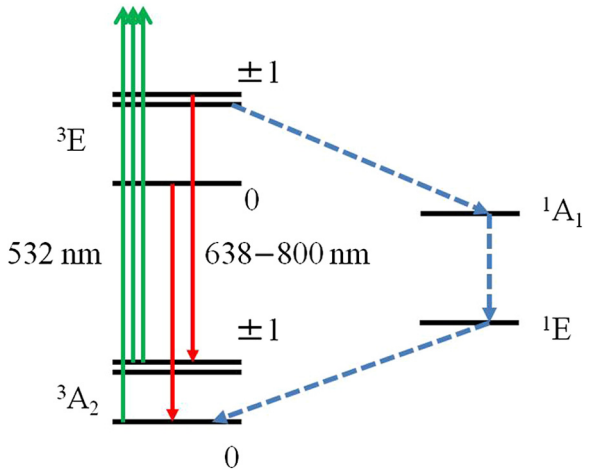

FIG. 1. Energy-level diagram of a NV center. $^3A_2$ is the spin-triplet ground state and ^3E is the excited state. $^1A_1$ and ^1E are the singlet states. Dashed blue line denotes the nonradiative decay path.

The NV center Hamiltonian, which contains the effects of the temperature, magnetic fields, and electric field, is expressed as

$$\begin{aligned} H &= D_g(T,\varepsilon_z)S_z^2 + g_e\mu_B B_z S_z + g_e\mu_B(B_x S_x + B_y S_y) \\ &+ c_{\varepsilon_\perp}\epsilon_x(S_x^2 - S_y^2) + c_{\varepsilon_\perp}\varepsilon_y(S_x S_y + S_y S_x) \\ &+ \lambda\cos(\varpi t)S_x + A_{||}S_z I_z + \frac{A_\perp}{2}(S_+ I_- + S_- I_+) \\ &+ P\left(I_z^2 - \frac{1}{3}I^2\right) - g_n\mu_N B_z I_z, \end{aligned}$$

where S (I) is a spin-1 operator of the electron (nuclear) spin, $\epsilon_{x(y)}$ is a term to represent strain (electric) fields along the x or y axis, $g_e\mu_B B_z S_z$ ($g_n\mu_N B_z I_z$) is the Zeeman term of the electron (nuclear) spin, λ is the microwave amplitude, ω is the microwave driving frequency, P is the quadrupole splitting, $A_{||}(A_\perp)$ is the parallel (perpendicular) hyperfine coupling, $c_{\varepsilon_\perp} = 2\pi \times 170$ kHz/(V μm), and

$$D(T,\varepsilon_z) = 2\pi \times 2870.685\ \text{MHz} + C_T\Delta T + c_{\varepsilon_{||}}\varepsilon_z,$$

where $C_T = 2\pi \times (-78.6 \pm 0.5$ kHz/K) and $c_{\varepsilon_{||}} = 2\pi \times 3.5$ kHz/(V μm). Since the equation contains the terms $g_e\mu_B(= 2\pi \times 28.7$ GHz/T), $c_{\varepsilon_\perp}$, and C_T, the resonant frequencies in the ODMR spectrum depend on the magnetic field, electric field, and temperature. Here, the x axis is defined as parallel to the direction of the applied microwave pulses, while the z axis is parallel to the NV center axis. Although $c_{\varepsilon_{||}}$ and $g_n\mu_N(= 2\pi \times 3.08$ MHz/T) have finite contributions to the ODMR signal, their effects are much smaller. Consequently, they are ignored in this paper.

The uncertainty of an estimated parameter with a diamond-based sensor is given by

$$\partial S_{\min} \sim \frac{1}{(|\partial P_{\text{signal}}/\partial S_m|_{\max}\sqrt{N})},$$

where S_m is the amplitude of the target parameter (temperature, electric field, or magnetic field) and P_{signal} is the optical signal intensity from the NV center. This formula shows that the sensitivity can be increased by increasing either the gradient of the ODMR signal or the number of NV centers. However, as the concentration of the NV centers increases, noise effects such as inhomogeneous magnetic fields, strain (electric field) variations, and homogeneous broadening tend to be larger, increasing the linewidth in the ODMR signal. This means that there is a trade-off relationship between $|\partial P_{\text{signal}}/\partial S_m|_{\max}$ and N. Thus, it is not trivial to find the optimized concentration of NV centers for high-performance sensing devices. This motivated us to understand the influence of NV centers on the noise parameters.

It was previously revealed that the ODMR spectrum of a high-density ensemble of NV centers shows a sharp-dip structure around 2870 MHz without an applied magnetic field. This cannot be fitted by the sum of Lorentzian functions [22]. Zhu *et al.* [22] successfully reproduced this sharp-dip structure using a theoretical model that contained the effects of inhomogeneous magnetic fields, inhomogeneous strain (electric field) distributions, and the homogeneous width of the NV centers. Matsuzaki *et al.* [28] showed that the sharp-dip structure is robust against inhomogeneous magnetic fields and strain (electric field) variations, but it is sensitive to homogeneous broadening. They introduced a schematic way to estimate the noise parameters of the NV centers from the fitting of the ODMR spectra.

In this paper, we use the scheme of Matsuzaki *et al.* to estimate the noise parameters of the NV centers in several diamond samples and demonstrate the dependence of the noise parameters on the spin concentration. Although there are many qualitative discussions about the dependence of the noise parameters on the spin concentration [28–31], the aim of this paper is to quantitatively analyze the dependence by comparing theory and experiment. In particular, we reveal the relationship between the NV center concentration and the strain (electric field) distribution.

As an application of our analysis, we discuss the sensitivity at high concentrations of the NV center ensemble as a temperature sensor. Our analysis provides a way to estimate the change in the noise parameters as a function of the NV center concentration. Then the dependence is simulated for each NV center ensemble concentration. By calculating the sensitivity at each concentration, we estimate the optimized density of the NV centers for the

minimum sensitivity. We propose using the dip structure in the ODMR spectrum, where the gradient around the dip structure becomes three times larger than that used for a temperature sensor in previous research. We compare the sensitivity of our scheme using the dip structure with that of the conventional scheme. Finally, we demonstrate that our scheme using a NV ensemble has the potential to provide a better temperature sensor.

This article is structured as follows. Section II describes the sample fabrication and the measurement setup. Section III details the theoretical model. Section IV presents the ODMR results for several diamond samples, the noise-parameter dependences, and the theoretical estimation of the temperature sensitivity of the NV centers. Section V summarizes the results.

II. EXPERIMENTAL METHOD

Diamonds, including substitutional nitrogen (P1) centers, are synthesized by high-pressure, high-temperature (HPHT) processes. The NV centers are prepared by electron irradiation and subsequent annealing at 1000 °C for 1 h in Ar gas. Afterwards, the diamonds are cleaned in a mixture of boiling acids (1:1 sulfuric acid and nitric acid) to remove graphitic carbon and oxygen termination at the surface. The P1-center concentrations are investigated by electron paramagnetic resonance (EPR) spectroscopy at room temperature, while the NV center concentrations are investigated by the fluorescence intensity when a 532-nm laser is applied. The diamonds are measured by ODMR spectroscopy with use of a laboratory-built confocal microscope at room temperature. It is possible to initialize and read out the NV centers by illumination with a green laser (532-nm) pulse (100 μs) of 50 μW.

Microwave pulses are generated via a copper wire, which is placed close to the diamond surface. This setup allows the NV centers to be controlled. The NV centers have a Rabi frequency, Ω, of $2\pi \times 125$ kHz for a pulse duration of around 4 μs. To apply an external magnetic field, we use a permanent magnet. Suitable magnetic fields are applied on the diamonds, inducing a separation of the ODMR signals into four groups with different crystallographic axes in the diamond lattice.

III. MODEL

We introduce a model to simulate the ODMR spectra [28]. The Hamiltonian of the NV center is described as

$$H = DS_z^2 + g_e\mu_B B_z S_z + E_1(S_x^2 - S_y^2) + E_2(S_xS_y + S_yS_x) + \lambda\cos(\varpi t)S_x,$$

where $E_1 = c_{\varepsilon_\perp}\epsilon_x$ and $E_2 = c_{\varepsilon_\perp}\varepsilon_y$. The x and y components of the magnetic fields are negligible because the Zeeman energy is assumed to be much smaller than the zero-field splitting (D). Since we consider the NV center ensemble, the total Hamiltonian in a rotating frame, which is defined by $U = e^{-i\omega S_z^2 t}$, is described as

$$\begin{aligned} H &\sim \hbar\sum_{k=1}^{N}\Big[(D_k-\omega)S_{z,k}^2 + E_1^{(k)}(S_{x,k}^2 - S_{y,k}^2) \\ &\quad + E_2^{(k)}(S_{x,k}S_{y,k} + S_{y,k}S_{x,k}) + g_e\mu_B B_z^{(k)}S_z + \frac{\lambda}{2}S_x^{(k)}\Big] \\ &= \hbar\sum_{k=1}^{N}\Big[(D_k-\omega)(|B\rangle_k\langle B| + |D\rangle_k\langle D|) + E_1^{(k)}(|B\rangle_k\langle B| \\ &\quad - |D\rangle_k\langle D|) + iE_2^{(k)}(|B\rangle_k\langle D| - |D\rangle_k\langle B|) \\ &\quad + g_e\mu_B B_z^{(k)}E_2^{(k)}(|B\rangle_k\langle D| + |D\rangle_k\langle B|) \\ &\quad + \frac{\lambda}{2}(|0\rangle_k\langle B| + |B\rangle_k\langle 0|)\Big], \end{aligned}$$

where $|B_k\rangle = (1/\sqrt{2})(|1\rangle_k + |-1\rangle_k)$ and $|D\rangle_k = (1/\sqrt{2})(|1\rangle_k - |-1\rangle_k)$. By assuming that D_k, $B_z^{(k)}$, $E_1^{(k)}$, and $E_2^{(k)}$ are randomly distributed, one can include the effect of the inhomogeneous broadening. More specifically, the random distributions of D_k, $E_1^{(k)}$, and $E_2^{(k)}$ are described by a Lorentzian function. The inhomogeneous strain (electric field) distribution along the z axis included in D_k is set to 1/50 of the magnitude of the inhomogeneous strain (electric field) distribution along the x and y axes because $c_{\varepsilon_\parallel}$ is 50 times smaller than $c_{\varepsilon_\perp}$ [16]. The effect of other nuclear spins (^{15}N, ^{13}C) is considered as the effect of randomized magnetic fields on the electron spin. P1 centers are also the sources of the randomized magnetic fields. In this model, we include these effects by a Lorentzian probability distribution of the magnetic fields applied on the NV centers. The hyperfine interaction from the nitrogen nuclear spins induces an effective magnetic field on the NV centers. This leads to a random distribution of the magnetic fields ($B_z^{(k)}$). In our experimental conditions, the nitrogen nuclear spin in the NV becomes a completely mixed state, which means that the state of the nitrogen nuclear spin is $|-1\rangle$, $|0\rangle$, or $|1\rangle$ with an equal probability distribution. Depending on the state of the nitrogen nuclear spin, the effective magnetic fields on the NV centers are different. This means that we can consider the distribution as Lorentzian functions, which are separated by $2\pi \times 2.3$ MHz, because the state of the nuclear spin become almost completely mixed at room temperature. Such a theoretical model was used to reproduce experimental results for an ensemble of NV centers by many researchers [22–24,28].

To include the effect of the homogeneous broadening [28], we adopt a Lindblad-type master equation, which is

expressed as

$$\frac{d\rho(t)}{dt} = -\frac{i}{\hbar}[H,\ \rho(t)] + \sum_{k=1}^{N}\sum_{j=1}^{4}\gamma_{j,k}[2L_{j,k}\rho(t)L_{j,k}^{\dagger} - L_{j,k}^{\dagger}L_{j,k}\rho(t) - \rho(t)L_{j,k}^{\dagger}L_{j,k}],$$

where $\gamma_{j,k}$ $(j = 1, 2, 3, 4)$ is the decay rate and $L_{j,k}$ $(j = 1, 2, 3, 4)$ is the Lindblad operator. In the case of NV centers, $L_{1,k} = |B\rangle_k\langle D|$, $L_{2,k} = |D\rangle_k\langle B|$, $L_{3,k} = |0\rangle_k\langle B|$, and $L_{4,k} = |0\rangle_k\langle D|$, where $\gamma_{1,k} = \gamma_{2,k} = \Gamma$ is the dephasing rate of the high-frequency magnetic field noise and $\gamma_{3,k} = \gamma_{4,k} = \Gamma'$ is the energy relaxation rate. Since the NV center has an energy relaxation time much longer than the dephasing time, as described later, the limit of the small energy relaxation rate is used. Additionally, we assume a steady state. Hence, the time derivative of $\rho(t)$ can be set as zero. Moreover, to avoid power broadening, the microwave strength λ is considered to be much smaller than the other parameters. From these assumptions, an analytical solution of the master equations can be obtained [28]:

$$\begin{aligned} P_0 &= 1 - \frac{1}{N}\sum_{k=1}^{N}\mathrm{Tr}[\rho(\infty)|0><0|], \\ &= 1 - \frac{1}{N}\left[\sum_{k=1}^{N}\left|\frac{\lambda'(\varpi - \varpi_d^{(k)} + i\Gamma'')}{(\varpi - \varpi_b^{(k)} + i\Gamma'')(\varpi - \varpi_d^{(k)} + i\Gamma'') - (|J_k|^2 + |J_k'|^2)}\right|^2 \right. \\ &\quad \left. + \left|\frac{\lambda'(J_k - iJ_k')}{(\varpi - \varpi_b^{(k)} + i\Gamma'')(\varpi - \varpi_d^{(k)} + i\Gamma'') - (|J_k|^2 + |J_k'|^2)}\right|^2\right], \end{aligned}$$

where $\varpi_b^{(k)} = D_k - E_1^{(k)}$, $\varpi_d^{(k)} = D_k + E_1^{(k)}$, $J_k = g\mu_B B_z^{(k)}$, $J_k' = E_2^{(k)}$, $\Gamma'' = \Gamma + \Gamma'$, and $\lambda' = \sqrt{(\Gamma''/\Gamma')}\lambda$. We take the limit of a small energy relaxation rate Γ', while keeping λ' constant. The higher-order terms of λ' are dropped because the microwave driving is assumed to be sufficiently weak. Thus,

$$\begin{aligned} P_0 &= 1 - \frac{1}{N}\left[\sum_{k=1}^{N}\left|\frac{\lambda'(\varpi - \varpi_d^{(k)} + i\Gamma)}{(\varpi - \varpi_b^{(k)} + i\Gamma)(\varpi - \varpi_d^{(k)} + i\Gamma) - (|J_k|^2 + |J_k'|^2)}\right|^2 \right. \\ &\quad \left. + \left|\frac{\lambda'(J_k - iJ_k')}{(\varpi - \varpi_b^{(k)} + i\Gamma)(\varpi - \varpi_d^{(k)} + i\Gamma) - (|J_k|^2 + |J_k'|^2)}\right|^2\right]. \end{aligned}$$

This approach can reproduce the ODMR spectra with high NV center concentrations.

IV. RESULTS AND DISCUSSION

Table I shows P1, NV, and spin concentrations (which are the sum of the P1 and NV concentrations) for the four diamond samples estimated from the EPR and fluorescence measurements. Fitting our numerical simulation to the ODMR spectra of the samples determines the noise parameters of the samples. Figures 2(a), (c), (e), and (g) show the ODMR simulation results without an external magnetic field and Figs. 2(b), (d), (f), and (h) show the ODMR simulation results with an external magnetic field. In the simulation, we change the parameters $\Gamma/2\pi$ (homogeneous broadening), $dg\mu B_z/2\pi$ (inhomogeneous magnetic fields), and $dE_{1,2}/2\pi$ [inhomogeneous strain (electric field) distribution]. All other parameters are fixed. The sharp dip in the ODMR spectrum strongly depends on $\Gamma/2\pi$, but the dip structure is insensitive to the change in

TABLE I. P1 center concentration and NV center concentration of the four HPHT samples.

Sample	P1 center concentration (10^{17}/cm^3)	NV center concentration (10^{17}/cm^3)
1	3.3	1.2
2	3.6	5.2
3	5	10
4	33.6	9.2

$dg\mu B_z/2\pi$ and $dE_{1,2}/2\pi$. Consequently, $\Gamma/2\pi$ can be estimated from the shape of the sharp dip. Strictly speaking, there must be an effect of Earth's magnetic field (of around 0.045 mT) on the NV centers, even when experimentalists did not apply any external magnetic fields. However, by numerical simulations, we check that the effect of Earth's magnetic field is negligibly small in the ODMR spectrum, and the existence of Earth's magnetic field does not qualitatively change our results (Fig. 3).

The ODMR signal in an external magnetic field is broadened mainly by the contribution of $dg\mu B_z/2\pi$, but it is robust against $dE_{1,2}/2\pi$. Hence, $dg\mu B_z/2\pi$ can be estimated from the ODMR width in an external magnetic field. Since the above approach can estimate both $\Gamma/2\pi$ and $dg\mu B_z/2\pi$, $dE_{1,2}/2\pi$ can also be estimated from the ODMR spectrum without an external magnetic field, where $\Gamma/2\pi$ and $dg\mu B_z/2\pi$ have already been determined from other simulation results.

The parameters strongly depend on the spin concentration. Figure 4 plots the estimated parameters (obtained from the fitting) as functions of the spin concentration. $dg\mu B_z/2\pi$ (HWHM) [Fig. 4(a)] and $\Gamma/2\pi$ (HWHM) [Fig. 4(b)] nearly linearly depend on the spin concentration, whereas $dE_{1,2}/2\pi$ (HWHM) [Fig. 4(c)] nearly linearly depends on the NV center concentration. The P1 center is considered as an electron spin bath that affects both the inhomogeneous magnetic fields and the high-frequency magnetic field noises. Not only the strain distribution but also the inhomogeneous electric fields can contribute to $dE_{1,2}/2\pi$. Electron irradiation induces defects, which may lead to the strain distribution [1]. The NV centers have a negative charge, and the same amount of P1 centers have a positive charge after donation of an electron to the NV centers, which may cause the inhomogeneous electric fields.

Using knowledge of the dependences of the noise parameters on the NV concentrations created by electron irradiation in the HPHT diamond samples, one can theoretically simulate the ODMR spectra as the NV center concentration changes. This is especially important to optimize the NV center concentration to realize high-performance quantum devices. As an example, here the case where the NV center is used as a temperature sensor is considered and the optimized NV center concentration is theoretically predicted to maximize the sensitivity. In the estimated temperature sensitivity, an ideal condition where only the NV centers have electron spins in diamond is considered.

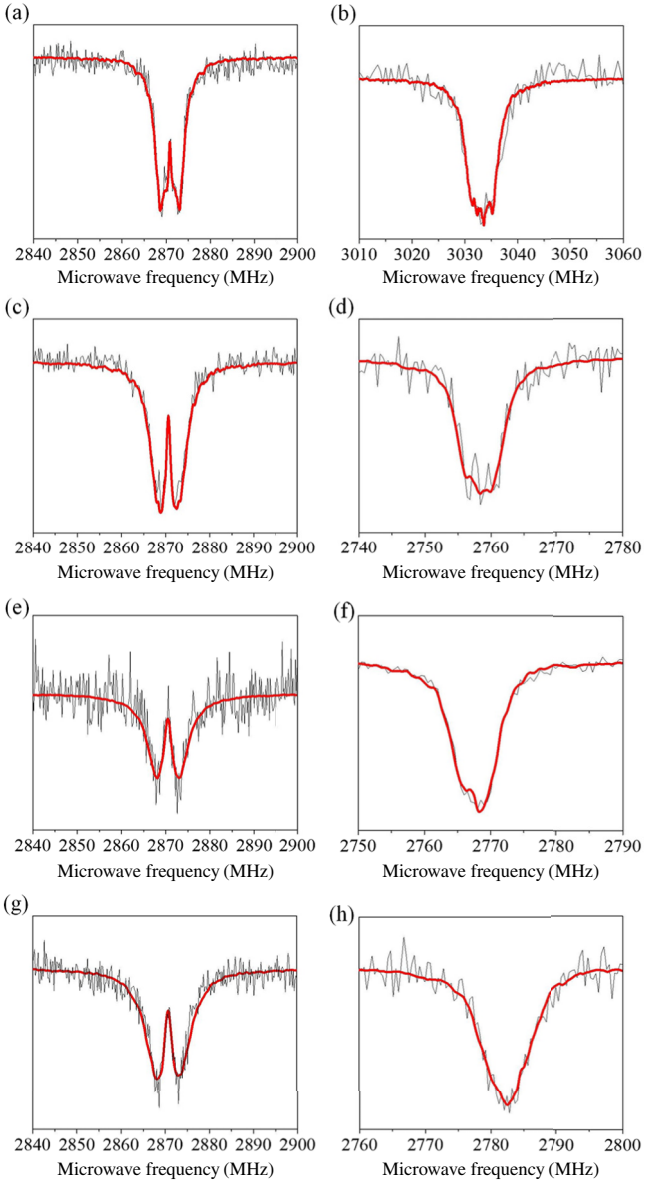

FIG. 2. ODMR simulation results for (a),(b) sample 1, (c),(d) sample 2, (e),(f) sample 3, and (g),(h) sample 4. External magnetic fields are not applied for (a), (c), (e), and (g), while external magnetic fields are applied for (b), (d), (f), and (h). The black line is the experimental result and the red line is the numerical result. Without the external magnetic field, a sharp-dip structure is clearly observed around 2.87 GHz. On the other hand, with the external magnetic field, only the normal-peak structure is observed around resonant frequencies.

In the ideal condition, diamond has equal amounts of P1 centers and NV centers, but the P1 centers have positive charge states. The positive charge state of the P1

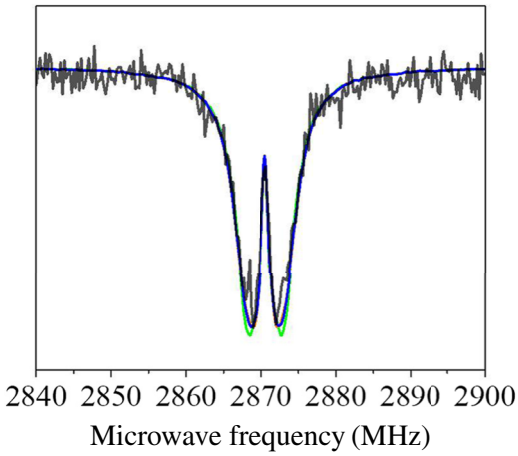

FIG. 3. Simulation results including Earth's magnetic field. We assume that the amplitude of Earth's magnetic field is 0.045 mT. The black line shows the experimental result for sample 2. The green line shows the simulation result without Earth's magnetic field. The gray line shows the simulation result with Earth's magnetic field in the (111) direction, and the red line shows the simulation result with Earth's magnetic field in the (100) direction. The blue line shows the simulation result with Earth's magnetic field in the direction with polar coordinates $\theta = 30°$, $\phi = 60°$.

center has no electron spin. Additionally, the magnitude of the inhomogeneous strain (electric field) distribution in the z-direction is 50 times smaller than that in the perpendicular direction [16]. Here, the microwave power is fixed as an experimentally realizable value in our laboratory; that is, $\lambda/2\pi = 0.29$ MHz. The sensing volume is assumed to be around 0.1 μm^3, which is determined by the diffraction-limited detection volume of our confocal microscopy. The estimated temperature sensitivity from the ODMR spectrum is given by

$$\eta = \frac{\sigma}{C_{\max} C_T} \frac{1}{\sqrt{1/TN}} \frac{1}{\sqrt{\mathrm{OD_{ND}}}},$$

where σ is the standard deviation of our measurement system at room temperature obtained with sample 4 (when we drive the system with off-resonant microwave pulses), $C_{\max}$ is the maximum gradient of the estimated ODMR spectrum, $C_T = 78.6$ kHz/K is the temperature dependence of the zero-field splitting, T is the measurement time, N is the proportion of the NV center concentration of the sample to that of sample 4, and $\mathrm{OD_{ND}}$ (=6000) is the fluorescence intensity blocked a neutral-density filter.

To measure the temperature with the NV center via the ODMR spectra, either the sharp-dip structure without an applied magnetic field or a normal-peak structure with an applied magnetic field is suitable. Although the latter method is more common in previous experimental demonstrations of diamond-based quantum sensors, the former may be more suitable for some applications due to the large gradient with respect to the small change in the microwave frequency. Here, when the normal-peak structure is used, the magnetic fields are assumed to be applied exactly along the [001] direction. Hence, every NV center has the same resonant frequency. This is an important assumption to increase the sensitivity when the peak structure is used. Otherwise, only some of the NV centers can be controlled by the resonant microwave pulses for the sensing. (On the other hand, when the dip structure is used, every NV center can be naturally involved in the sensing process without such a careful magnetic field alignment. This is one advantage of the dip structure.)

Figure 5 plots the numerically estimated temperature sensitivity with respect to the NV center concentration. The black squares represent the sensitivity obtained with the sharp-dip structure without an applied magnetic field. The red squares represent the sensitivity obtained with the peak structure observed in the normal ODMR spectrum under an external magnetic field applied exactly along the [001] direction. The blue squares show the results for the normal ODMR spectrum with a magnetic field in an arbitrary direction for one of the four NV axes. (Each ensemble has four NV axes. Thus, in the case of a magnetic field in an arbitrary direction, four resonance frequencies are present.) The approach using the sharp-dip structure has about a threefold greater temperature sensitivity than the approach using the peak structure under an external magnetic field applied exactly along the [001] direction. The estimated optimal sensitivity is around 0.76 mK/$\sqrt{\mathrm{Hz}}$ at room temperature with an NV center concentration of

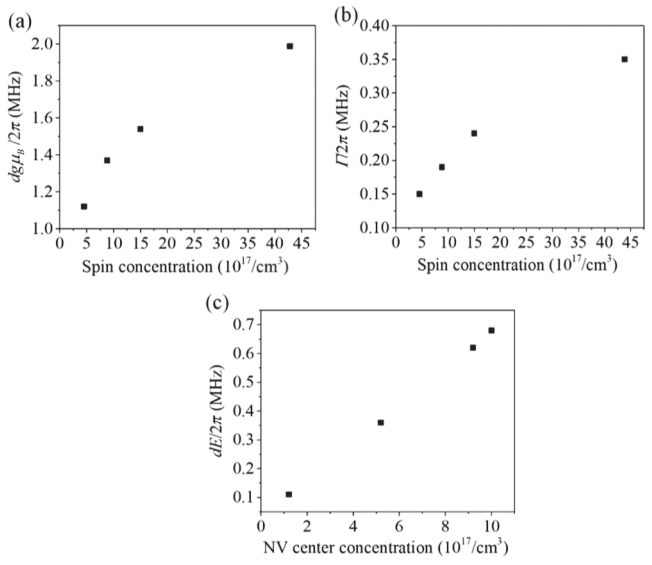

FIG. 4. (a) $dg\mu_B/2\pi$ (HWHM), (b) $\Gamma/2\pi$ (HWHM), and (c) $dE/2\pi$ (HWHM) with respect to spin (NV center) concentration. The parameters are estimated by fitting the numerical simulations to the experimental results.

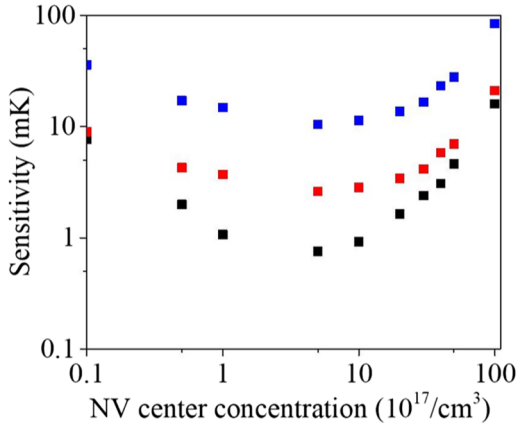

FIG. 5. Numerically estimated sensitivity with respect to the NV concentration with low-microwave-power ODMR. Black squares represent the sensitivity of the approach using the sharp-dip structure without an applied magnetic field. Red squares represent the sensitivity of the approach using the peak structure observed in the normal ODMR spectrum under an external magnetic field applied exactly along the [001] direction. Blue squares represent the results obtained with the peak structure observed in the normal ODMR spectrum with an arbitrary direction of the magnetic field and when the ODMR signal of only one of the four NV axes is measured.

$5.0 \times 10^{17}/\mathrm{cm}^3$. Our theoretical estimation of the sensitivity is almost 1 order of magnitude greater than the currently reported value (5 mK/$\sqrt{\mathrm{Hz}}$), which was achieved with a confocal microscope with a NV center [12,13].

Although there are many ways to optimize the performance of the sensors, we especially focus on the concentration of the NV centers for the optimization. Increasing the sensing volume V in the bulk diamond, which is equivalent to increasing the number of measured NV centers, can increase the sensitivity by a factor of $\sqrt{V}$. If the sensing volume is assumed to be around 1000 μm^3, the estimated temperature sensitivity achieved is approximately 20 μK/$\sqrt{\mathrm{Hz}}$. Increasing the averaging time and/or decreasing the measurement standard deviation (possibly by use of magnetic shielding) should also help to increase the sensitivity. Furthermore, it should be noted that our estimation considers a relatively low microwave power (below 10 mG) in the ODMR signal. Such low-power microwave driving is important when one is measuring biomaterials to avoid heating the water. Additionally, such a low-power drive prevents heating of the target sample (the object whose temperature is measured), which is one of the reasons for the deteriorated performance of a previous temperature sensor [13]. In principle, our optimization is useful for sensing not only at room temperature but also at high temperature. However, in the case of high temperature (400–700 K), the ODMR contrast and fluorescence intensity decrease [32], and so our estimated sensitivity becomes lower. Therefore, our estimated sensitivity can be achieved at around room temperature.

V. CONCLUSION

We investigate the dependence of the noise parameters of high-density NV center ensembles. Inhomogeneous magnetic fields and homogeneous broadening are nearly linearly dependent on the spin concentrations, whereas the inhomogeneous strain (electric field) distribution is nearly linearly dependent on the NV center concentration. Additionally, to illustrate the importance of such parameter dependences when one is optimizing a quantum device, we theoretically estimate the influence of spin concentration on the performance of the NV center ensemble as a temperature sensor. On the basis of the theoretical calculations, the sharp-dip structure in the ODMR spectrum is suitable for a temperature sensor. The optimal sensitivity is predicted to occur at around 0.76 mK/$\sqrt{\mathrm{Hz}}$ with a NV center concentration of $5.0 \times 10^{17}/\mathrm{cm}^3$ and a spatial resolution of approximately 0.1 μm^3, which is the diffraction-limited volume in a typical confocal microscope. This estimated value is better than the previous experimental results [12,13]. Our results are essential to control and use NV center ensembles as high-performance quantum devices, particularly as temperature sensors.

ACKNOWLEDGMENTS

This work was supported by KAKENHI (Grants No. 15H05868, No. 15H05870, and No. 15K17732) and CREST (Grant No. JPMJCR1333).

[1] G. Davies and H. M. Hamer, Optical studies of the 1.945 eV vibronic band in diamond, Proc. R. Soc. Lond. Ser. A Math. Phys. Eng. Sci. **348**, 285 (1976).

[2] A. Gruber, A. Dräbenstedt, C. Tietz, L. Fleury, J. Wrachtrup, and C. V. Borczyskowski, Scanning confocal optical microscopy and magnetic resonance on single defect centers, Science **276**, 2012 (1997).

[3] F. Jelezko, T. Gaebel, I. Popa, A. Gruber, and J. Wrachtrup, Observation of Coherent Oscillations in a Single Electron Spin, Phys. Rev. Lett. **92**, 076401 (2004).

[4] M. W. Doherty, N. B. Manson, P. Delaney, F. Jelezko, J. Wrachtrup, and L. C. L. Hollenberg, The nitrogen-vacancy colour centre in diamond, Phys. Rep. **528**, 1 (2013).

[5] T. Shimo-Oka, H. Kato, S. Yamasaki, F. Jelezko, S. Miwa, Y. Suzuki, and N. Mizuochi, Control of coherence among the spins of a single electron and the three nearest neighbor ^{13}C nuclei of a nitrogen-vacancy center in diamond, Appl. Phys. Lett. **106**, 153103 (2015).

[6] P. Neumann, N. Mizuochi, F. Rempp, P. Hemmer, H. Watanabe, S. Yamasaki, V. Jacques, T. Gaebel, F. Jelezko, and J. Wrachtrup, Multipartite entanglement among single spins in diamond, Science **320**, 1326 (2008).

[7] T. A. Wolf, P. Neumann, K. Nakamura, H. Sumiya, T. Ohshima, J. Isoya, and J. Wrachtrup, Subpicotesla Diamond Magnetometry, Phys. Rev. X **5**, 041001 (2015).
[8] N. Aslam, M. Pfender, P. Neumann, R. Reuter, A. Zappe, F. F. D. Olivelea, A. Denisenko, H. Sumiya, S. Onoda, J. Isoya, and J. Wrachtrup, Nanoscale nuclear magnetic resonance with chemical resolution, Science **357**, 67 (2017).
[9] J. M. Boss, K. S. Cujia, J. Zopes, and C. L. Degen, Quantum sensing with arbitrary frequency resolution, Science **356**, 837 (2017).
[10] S. Schmitt, T. Gefen, F. M. Sturner, T. Unden, G. Wolff, C. Muller, J. Scheuer, B. Naydenov, M. Markham, S. Pezzagna, J. Meijer, I. Sehwarz, M. Plenio, A. Retzker, L. P. McGuinness, and F. Jelezko, Submillihertz magnetic spectroscopy performed with a nanoscale quantum sensor, Science **356**, 832 (2017).
[11] H. A. Clevenson, M. E. Trusheim, C. A. Teale, T. Schröder, D. A. Braje, and D. R. Englund, Broadband magnetometry and temperature sensing with a light trapping diamond waveguide, Nat. Phys. **11**, 393 (2015).
[12] P. Neumann, I. Jakobi, F. Dolde, C. Burk, R. Reuter, G. Waldherr, J. Honert, T. Wolf, A. Brunner, J. H. Shim, D. Suter, H. Sumiya, J. Isoya, and J. Wrachtrup, High-precision nanoscale temperature sensing using single defects in diamond, Nano Lett. **13**, 2738 (2013).
[13] G. Kucsko, P. C. Maurer, N. Y. Yao, M. Kubo, H. J. Noh, P. K. Lo, H. Park, and M. D. Lukin, Nanometre-scale thermometry in a living cell, Nature **500**, 12373 (2013).
[14] T. Plakhotnik, M. W. Doherty, J. H. Cole, R. Chapman, and N. B. Manson, High-precision nanoscale temperature sensing using single defects in diamond, Nano Lett. **14**, 4990 (2014).
[15] M. W. Doherty, V. V. Struzhkin, D. A. Simpson, L. P. McGuinness, Y. Meng, A. Stacey, T. J. Karle, R. J. Hemley, N. B. Manson, L. C. L. Hollenberg, and S. Prawer, Electronic Properties and Metrology Applications of the Diamond NV^- Center under Pressure, Phys. Rev. Lett. **112**, 047601 (2014).
[16] F. Dolde, H. Fedder, M. W. Doherty, T. Nobauer, F. Rempp, G. Balasubramanian, T. Wolf, F. Reinhard, L. C. Hollenberg, F. Jelezko, and J. Wrachtrup, Electric-field sensing using single diamond spins, Nat. Phys. **7**, 459 (2011).
[17] F. Dolde, M. W. Doherty, J. Michl, I. Jakobi, B. Naydenov, S. Pezzagna, J. Meijer, P. Neumann, F. Jelezko, N. B. Manson, and J. Wrachtrup, Nanoscale Detection of a Single Fundamental Charge in Ambient Conditions Using the NV^- Center in Diamond, Phys. Rev. Lett. **112**, 097603 (2014).
[18] E. Bourgeois, A. Jarmola, P. Siyushev, M. Gulka, J. Hruby, F. Jelezko, D. Budker, and M. Nesládek, Photoelectric detection of electron spin resonance of nitrogen-vacancy centres in diamond, Nat. Commun. **6**, 9577 (2015).
[19] G. Balasubramanian, P. Neumann, D. Twitchen, M. Markham, R. Kolesov, N. Mizuochi, J. Isoya, J. Achard, J. Beck, J. Tissler, V. Jacques, P. R. Hemmer, F. Jelezko, and J. Wrachtrup, Ultralong spin coherence time in isotopically engineered diamond, Nat. Mater. **8**, 383 (2009).
[20] N. Mizuochi, P. Neumann, F. Rempp, J. Beck, V. Jacques, P. Siyushev, K. Nakamura, D. J. Twitchen, H. Watanabe, S. Yamasaki, F. Jelezko, and J. Wrachtrup, Coherence of single spins coupled to a nuclear spin bath of varying density, Phys. Rev. B **80**, 041201(R) (2009).
[21] T. Yamamoto, T. Umeda, K. Watanabe, S. Onoda, M. L. Markham, D. J. Twitchen, B. Naydenov, L. P. McGuinness, T. Teraji, S. Koizumi, F. Dolde, H. Fedder, J. Honert, J. Wrachtrup, T. Ohshima, F. Jelezko, and J. Isoya, Extending spin coherence times of diamond qubits by high-temperature annealing, Phys. Rev. B **88**, 075206 (2013).
[22] X. Zhu, Y. Matsuzaki, R. Amsuss, K. Kakuyanagi, T. Shimo-oka, N. Mizuochi, K. Nemoto, K. Semba, W. J. Munro, and S. Saito, Observation of dark states in a superconductor diamond quantum hybrid system, Nat. Commun. **5**, 3524 (2014).
[23] Y. Matsuzaki, X. Zhu, K. Kakuyanagi, H. Toida, T. Shimooka, N. Mizuochi, K. Nemoto, K. Semba, W. J. Munro, H. Yamaguchi, and S. Saito, Improving the lifetime of the nitrogen-vacancy-center ensemble coupled with a superconducting flux qubit by applying magnetic fields, Phys. Rev. A **91**, 042329 (2015).
[24] Y. Kubo, C. Grezes, A. Dewes, T. Umeda, J. Isoya, H. Sumiya, N. Morishita, H. Abe, S. Onoda, T. Ohshima, V. Jacques, A. Dréau, J.-F. Roch, I. Diniz, A. Auffeves, D. Vion, D. Esteve, and P. Bertet, Hybrid Quantum Circuit with a Superconducting Qubit Coupled to a Spin Ensemble, Phys. Rev. Lett. **107**, 220501 (2011).
[25] S. Choi, J. Choi, R. Landig, G. Kucsko, H. Zhou, J. Isoya, F. Jelezko, S. Onoda, H. Sumiya, V. Khemani, C. V. keyserlingk, N. Y. Yao, E. Demler, and M. D. Lukin, Observation of discrete time-crystalline order in a disordered dipolar many-body system, Nature **543**, 221 (2017).
[26] J. Choi, S. Choi, G. Kucsko, P. C. Maurer, B. J. Shields, H. Sumiya, S. Onoda, J. Isoya, E. Demler, F. Jelezko, N. Y. Yao, and M. D. Lukin, Depolarization Dynamics in a Strongly Interacting Solid-State Spin Ensemble, Phys. Rev. Lett. **118**, 093601 (2017).
[27] G. Kucsko, S. Choi, J. Choi, P. C. Maurer, H. Zhou, R. Landig, H. Sumiya, S. Onoda, J. Isoya, F. Jelezko, E. Demler, N. Y. Yao, and M. D. Lukin, Critical thermalization of a disordered dipolar spinsystem in diamond, arXiv:1609.08216.
[28] Y. Matsuzaki, H. Morishita, T. Shimo-oka, T. Tashima, K. Kakuyanagi, K. Semba, W. J. Munro, H. Yamaguchi, N. Mizuochi, and S. Saito, Optically detected magnetic resonance of high-density ensemble of NV^- centers in diamond, J. Phys.: Condens. Matter **28**, 275302 (2016).
[29] F. T. Charnock and T. A. Kennedy, Combined optical and microwave approach for performing quantum spin operations on the nitrogen-vacancy center in diamond, Phys. Rev. B 64, 041201R (2001).
[30] R. Hanson, V. V. Dobrovitski, A. E. Feiguin, O. Gywat, and D. D. Awshalom, Coherent dynamics of a single spin interacting with an adjustable spin bath, Science **320**, 352 (2008).
[31] G. D. Lange, Z. H. Wang, D. Ristè, V. V. Dobrovitski, and R. Hanson, Universal dynamical decoupling of a single solid-state spin from a spin bath, Science **330**, 60 (2010).
[32] D. M. Toyli, D. J. Christle, A. Alkauskas, B. B. Buckley, C. G. Van de Walle, and D. D. Awschalom, Measurement and Control of Single Nitrogen-Vacancy Center Spins above 600 K, Phys. Rev. X **2**, 031001 (2012).